Title
Throttle And Brake Control Systems For Automatic Vehicle Following

Authors
Ioannou, P.
Xu, Z.

Publication Date
1994

CALIFORNIA PATH PROGRAM
INSTITUTE OF TRANSPORTATION STUDIES
UNIVERSITY OF CALIFORNIA, BERKELEY

Throttle and Brake Control Systems for Automatic Vehicle Following

P. Ioannou
Z. Xu

University of Southern California

California PATH Research Paper

UCB-ITS-PRR-94-10

This work was performed as part of the California PATH Program of the University of California, in cooperation with the State of California Business, Transportation, and Housing Agency, Department of Transportation.

April 1994

ISSN 10551425

Throttle and Brake Control Systems for Automatic Vehicle Following *

P. Ioannou and **Z.** Xu
Southern California Center for
Advanced Transportation Technologies
EE - Systems, EEB 200B
University of Southern California
Los Angeles, CA 90089-2562

Abstract. **In this paper we present several throttle and brake control systems for automatic vehicle following. These control systems are designed and tested using a validated nonlinear vehicle model first and then actual vehicles. Each vehicle to be controlled is assumed to be equipped with sensors that, in addition to its own vehicle characteristics, provide measurements of the relative distance and relative speed between itself and the vehicle in front. Vehicle-to-vehicle communication required for the stability of the dynamics of a platoon of vehicles with desired constant intervehicle spacing is avoided. Instead stability is guaranteed by using a constant time headway policy and designing the control system for the throttle and brake appropriately. The proposed control systems guarantee smooth vehicle following even when the leading vehicle exhibits erratic speed behavior.**

1 Introduction

Advanced Vehicle Control Systems (AVCS) are important parts of Intelligent Vehicle Highway Systems (IVHS). The goal of AVCS is to introduce more automatic features in vehicles by using **sophisticated control systems, sensors and computers. These features may vary** from the simple cruise control system currently available in vehicles, to a fully automated vehicle where the driver and passengers are not part of the control system. Partially or fully automated vehicles may be part of system architectures that include the highways. Such architectures have been shown to have strong potential for dramatically increasing the capacity of freeways[1-5] and improving the smoothness of traffic flows [5].

An important component of AVCS is to design control systems for controlling the throttle and brake so that the vehicle can follow the speed response of the leading vehicle and at the same time keep a safe intervehicle spacing under the constraint of comfortable driving [6].

Studies on automatic vehicle following go as far back as **1970's** [7-8] where throttle and brake controllers were designed based on simple point mass vehicle models. More complicated vehicle models were used in the design of automatic vehicle following controllers in [6,9] where constant intervehicle spacing is desired at all speeds. In order to achieve platoon stability with desired constant intervehicle spacing, vehicle-to-vehicle communication was

***This work is supported by Caltrans through PATH of University of California and Ford Motor Company.**

shown to be necessary [9,10]. In [5], it was shown that under a constant time headway policy, the stability of the dynamics of a platoon of vehicles could be achieved without vehicle-to-vehicle communication, provided the throttle and brake controllers are designed appropriately.

In this paper we design and test three throttle controllers and one brake controller as well as the logic switch which governs the switching between throttle and brake control. The three throttle controllers are: a fixed gain Proportional-Integral-Derivative (PID) controller, a PID controller with gain scheduling, and an adaptive controller. Each vehicle to be controlled is assumed to be equipped with sensors which, in addition to its own vehicle characteristics such as vehicle speed, engine speed etc., provide measurements of the relative distance and relative speed between itself and the vehicle in front. The desired throttle angle and brake line pressure are directly calculated based on these sensor measurements. No vehicle-to-vehicle communication is assumed. A constant time headway policy is used to choose the desired intervehicle spacing. This policy, together with the appropriate design of the control system for throttle and brake, guarantees the stability of the dynamics of a platoon of vehicles. Tests of the proposed control systems are conducted using both a validated nonlinear vehicle model and an actual vehicle. The simulation and vehicle test results included in this paper show that the proposed control systems can achieve smooth, comfortable vehicle following even when the leading vehicle exhibits erratic speed behavior.

2 Longitudinal Vehicle Model

The block diagram of the longitudinal vehicle model is shown in Figure 1. This model was built based on physical laws and experimental data and was validated by experiments.

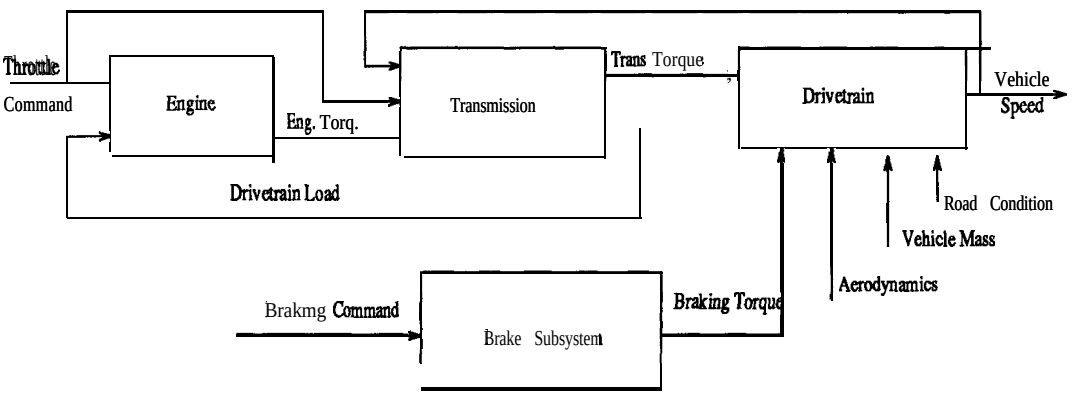

Figure 1: Longitudinal Vehicle Model

Each block can be considered as a subsystem with various inputs and outputs. The output of the engine subsystem is the engine torque that is a nonlinear function of the air/fuel ratio, the exhaust gas recirculation (EGR), the cylinder total mass charge, the spark advance, the engine speed and the drivetrain load as well as the throttle angle. The

spark advance, EGR, and air-to-fuel ratio are the outputs of an internal controller (inside the engine block of Fig.1) whose inputs are the throttle position, engine speed and drivetrain load.

The transmission subsystem is responsible for transferring engine torque to the drive-train depending on the vehicle speed and engine condition. The transmission considered in Figure 1 is an automatic transmission with hydraulic torque coupling and four forward transmission gears. For a certain gear state, the transmission torque output is a linear function of the engine torque. The gear state is a nonlinear function of the throttle angle, engine speed, and vehicle speed.

The drivetrain subsystem receives transmission torque and/or braking torque input and outputs vehicle speed, acceleration or deceleration. The vehicle speed and acceleration are affected by the road condition, aerodynamic drag and vehicle mass. The relationship between vehicle speed and transmission torque is also nonlinear.

The brake subsystem, which includes the brake actuator, receives braking commands and outputs braking torque. It behaves like a first order low pass filter [6] with some time delay. Based on experiments, we found that the time delay is noticeable only in the very beginning when the brake is applied and is very small later on. In addition, we also found from experiments that the dynamics of the brake subsystem are much faster than those of the drivetrain. In our design, both the time delay and the dynamics of the brake subsystem are ignored, leading to a constant gain relationship between the braking command input and braking torque output. In our simulations, however, the time delay and the dynamics of the brake subsystem are taken into account.

For longitudinal control, the system in Figure 1 may be considered as having two control input variables: throttle angle command and braking command, and one output: vehicle speed. The other inputs such as aerodynamic drag, road condition, and vehicle mass changes are treated as disturbances.

In our approach we separate the two input, one output system into a throttle angle to speed and braking command to speed subsystems. The reason for this is that in our approach the throttle and brake controllers are not allowed to act simultaneously. The throttle angle command is set to a minimum value whenever the braking command is sent to the brake actuator. The simplified models for the throttle and brake subsystems are developed in the following subsections.

2.1 Throttle Angle to Vehicle Speed and Position Model

As we mentioned before, the vehicle speed V is a nonlinear function of the throttle θ, i.e.,

$$v = F(\theta, t, \tau) \tag{1}$$

where $0 \leq \tau \leq t$ indicates the presence of dynamics. Since the model we have is very complicated and confidential, we are not presenting the detailed expression for $F(\theta, t, \tau)$. Expressions for $F(\theta, t, \tau)$ for various other vehicle models may be found in [6, 11, 12, 13]. The complexity of the model described above makes it difficult to design a controller directly

based on such a nonlinear model. In our approach we use linearization to obtain a linear model whose parameters are functions of operating points and use the simplified linear model to design the throttle controller. The controller designed, however, is tested on the actual nonlinear model. The linearization procedure is described as follows:

Let V_0 be the steady state vehicle speed for a throttle input θ_0. Define $\bar{V} \triangleq V - V_0$ as the deviation of the vehicle speed V from V_0, and $\bar{\theta} \triangleq \theta - \theta_0$ as the throttle deviation from θ_0. Using the validated nonlinear longitudinal vehicle model we find that, for any fixed gear state, the linearized model that relates $\bar{V}, \bar{\theta}$ over a wide range of speed V_0, i.e., from 0 to 36 m/s, has the form

$$\frac{\bar{V}}{\bar{\theta}} = \frac{b_0}{s^3 + a_2 s^2 + a_1 s + a_0} = \frac{b_0}{(s+p_1)(s+p_2)(s+p_3)} \tag{2}$$

where the coefficients b_0, a_0, a_1, a_2 are functions of the operating point (θ_0, V_0), i.e., b_0 and a_i have different values for different V_0 or θ_0.

For all operating points considered, however, we found that $b_0 > 0$, $p_1 > 0$, and p_2 and p_3 (which may be either conjugate complex or real numbers) have positive real parts. Furthermore, $Re(p_2), Re(p_3) >> p_1$ and $0 < p_1 \leq 0.2$. A measure of how far apart $Re(p_2)$ and $Re(p_3)$ are from p_1 can be given by the value of a variable μ defined as

$$\mu \triangleq \sup_{\theta_0 \in \Theta} \max \left[\frac{p_1}{Re(p_i)}, i = 2, 3 \right] \tag{3}$$

where Θ is the full change range of θ. Our simulation results show that $\mu < 0.05$ which indicates that $-p_1$ is the dominant pole and that fast modes associated with p_2 and p_3 can be neglected, leading to the simpler model

$$\frac{\bar{V}}{\bar{\theta}} = \frac{b}{s+a} \tag{4}$$

where a and b vary with V_0. The effects of the fast mode terms and uncertainties neglected in the linearization procedure may be modeled as a disturbance term d, leading to the model

$$\dot{\bar{V}} = -a\bar{V} + b\bar{\theta} + d \tag{5}$$

or equivalently,

$$\dot{V} = -a(V - V_0) + b\bar{\theta} + d. \tag{6}$$

In vehicle following, we consider vehicle speed as well as vehicle position. Adding the position variable X to the vehicle model, we obtain the complete dynamic equations of the throttle angle to vehicle speed and position subsystem

$$\begin{aligned} \dot{X} &= V \\ \dot{V} &= -a(V - V_0) + b\bar{\theta} + d. \end{aligned} \tag{7}$$

The above equations do not include the effect of braking torque on the vehicle speed V. They describe the dynamics of the throttle subsystem when the brake is off.

2.2 Braking Torque to Vehicle Speed and Position Model

Let us now assume that the throttle is at the minimum value that corresponds to idle engine speed. In this case the transmission torque is very small compared to the braking torque and is therefore neglected. The dynamic equations of the braking torque to vehicle speed and position subsystem are given as follows:

$$\begin{aligned} \dot{X} &= V \\ \dot{V} &= \tfrac{1}{M}(-c_1 T_b - f_0 - c_2 V - c_3 V^2) \end{aligned} \tag{8}$$

where T_b is the braking torque, M is the vehicle mass, $c_1 T_b$ is the braking force, f_0 represents the static friction force, $c_2 V$ represents the rolling friction force, $c_3 V^2$ represents the air resistant force and c_1, c_2, c_3, and f_0 are some known constants obtained from experiments. The above model is developed using Newton's second law of motion and is based on the assumption that the wheels of the vehicle are not locked. This assumption allows us to approximate the braking force as being proportional to the braking torque T_b [14].

3 Control Objectives

If we let subscripts l, f denote leading and following vehicle characteristics, the dynamic equations of vehicle following are:

$$\begin{aligned} \dot{X}_l &= V_l \\ \dot{X}_f &= V_f \\ \dot{V}_f &= \begin{cases} -a(V_f - V_0) + be, + d & \text{for throttle} \\ \tfrac{1}{M}(-c_1 T_b - f_0 - c_1 V_f - c_2 V_f^2) & \text{for brake.} \end{cases} \end{aligned} \tag{9}$$

One of the control objectives is to make $V_f \approx V_l$, i.e., V_l is considered to be the desired speed trajectory to be tracked by the following vehicle. We therefore take $V_0 = V_l$ thereafter. Defining relative speed $V_r \triangleq V_l - V_f$ and relative distance $X_r \triangleq X_l - X_r$, we obtain the following dynamic equations with X,. and V_f as the state variables:

$$\begin{aligned} \dot{X}_r &= V_l - V_f \\ \dot{V}_f &= \begin{cases} -a(V_f - V_l) + be, + d & \text{for throttle} \\ \tfrac{1}{M}(-c_1 T_b - f_0 - c_1 V_f - c_2 V_f^2) & \text{for brake.} \end{cases} \end{aligned} \tag{10}$$

Another control objective is to keep a desired intervehicle spacing S_d, measured from the front of the following vehicle to the rear of the leading vehicle. In our design, the desired intervehicle spacing S_d is chosen as

$$S_d = hV_f + S_0 \tag{11}$$

where h is known as the time headway, and $S_0 \geq 0$ is a constant. This policy for the desired intervehicle spacing is called constant time headway policy. As shown in [5], h can

be chosen based on the performance characteristics of the leading and following vehicles in a worst stopping scenario, the accuracy of sensors, etc. If we use δ to denote the deviation of the relative distance X_r from the desired spacing S_d, then we have

$$\delta = X_r - hV_f - S_0. \tag{12}$$

The overall control objective for vehicle following is to choose the throttle angle θ_f and braking torque T_b so that $\delta \to 0$ and $Vf \to V_l$. Due to ride comfort requirements, the control objective has to be achieved under the following constraints:

C1. $a_{min} \leq Vf \leq a_{max}$ where a_{min} and a_{max} are specified.

C2. The absolute value of jerk defined as $\ddot{V}_f$ should be as small as possible.

Note that among these two constraints, **C2** should be satisfied under the condition that **Cl** is satisfied. In other words, the controller has to first satisfy **Cl,** and then to satisfy ***c2.***

As mentioned in Section 1 the following vehicle is equipped with sensors that detect the relative speed V_r, relative distance X,., and its own speed ***Vf.*** From these measurements the velocity V_l of the leading vehicle can be calculated and is therefore known to the following vehicle.

The control system that can achieve the above objective may be divided into three parts: the throttle controller used when the brake is off; the brake controller used when the throttle controller is inactive; and the logic block which governs the switching between throttle and brake control actions. We treat each part of the overall control system separately in the following sections.

4 Throttle Control Design and Analysis

The dynamic equations of the throttle subsystem are

$$\begin{aligned} \dot{X}_r &= V_l - V_f \\ \dot{V}_f &= -a(V_f - V_l) + \textbf{be, } + \textbf{d} \\ \delta &= X_r - hV_f - S_0 \\ V_r &= V_l - V_f \end{aligned} \tag{13}$$

where $\bar{\theta}_f = \theta_f - \theta_0$ is to be chosen so that $V_r, \delta \to 0$ as $t \to \infty$. We propose three different controllers to generate θ_f. These are: a PID controller with fixed gains, a PID controller with gain scheduling, and an adaptive controller. We present and analyze each controller in the following subsections.

4.1 PID Controllers with Fixed Gain and Gain Scheduling

We propose the following controller for the throttle

$$\theta_f = \theta_0 + k_1 V_r + k_2 \delta + \int_0^t (k_3 V_r + k_4 \delta) d\tau. \tag{14}$$

This controller includes the term θ_0 that comes from a look-up table describing the relationship between θ_0 and the steady state vehicle speed V_0 which is taken to be equal to V_l, i.e.

$$\theta_0 = f^{-1}(V_l); \tag{15}$$

a proportional term $k_2\delta$; a "derivative" term $k_1 V_r$ and an integral action. The gains k_1 to k_4 are to be chosen to meet the control objective stated before. The use of $k_3 V_r + k_4 \delta$ instead of simply $k_4\delta$ in the integral action is found to be beneficial in reducing the speed overshoot due to large position error.

Substituting (14) into (13), we obtain the closed loop system

$$\begin{aligned} \dot{X}_r &= V_l - V_f \\ \dot{V}_f &= -(a + bk_1)(V_f - V_l) + bk_2\delta + b\textstyle\int_0^t (k_3 V_r + k_4\delta) d\tau + \boldsymbol{d} \\ \delta &= X_r - hV_f - S_0 \\ V_r &= V_l - V_f. \end{aligned} \tag{16}$$

It follows that

$$V_r = \frac{(s^2 + bhk_2 s + bhk_4)s}{\Delta(s)} V_l + \frac{b(k_2 s + k_4)s}{\Delta(s)} S_0 - \frac{s^2}{\Delta(s)} d \tag{17}$$

$$\delta = -\frac{[(1 - ah - bhk_1)s - bhk_3]s}{\Delta(s)} V_l - \frac{[s^2 + (a + bk_1)s + bk_3]s}{\Delta(s)} S_0 - \frac{(1 + hs)s}{\Delta(s)} d \tag{18}$$

where

$$\mathrm{A(s)} = s^3 + (a + bk_1 + bhk_2)s^2 + b(k_2 + k_3 + hk_4)s + bk_4. \tag{19}$$

The gains k_1 to k_4 can now be chosen so that the poles of the above transfer functions are in selected locations in the left half s-plane.

If d is constant or slowly time-varying, we will have sd ≈ 0 and d will have no or little effect on δ and V_r. Therefore, at steady state, $V_r = 0$ and $\delta = 0$ for constant V_l and S_0.

Let us now choose k_1 to k_4 so that

$$\Delta(s) = (s + \lambda_0)(s^2 + 2\zeta\omega_n s + \omega_n^2) \tag{20}$$

where $-\lambda_0$ is the desired real pole and ω_n, ζ are the natural frequency and damping ratio of the two desired complex poles, respectively. By comparing the coefficients of equal powers of s in (20), we have that

$$\begin{aligned} k_1 &= (\lambda_0 + 2\zeta\omega_n - bk_2 h - a)/b \\ k_3 &= (2\zeta\omega_n\lambda_0 + \omega_n^2 - bk_2 - h\lambda_0\omega_n^2)/b \\ k_4 &= \lambda_0\omega_n^2/b. \end{aligned} \tag{21}$$

Here k_2 can be chosen freely for pole placement purposes. From the analysis of the dynamics of a platoon of vehicles (see section 7), we choose

$$k_2 = 0.2/b \tag{22}$$

which simplifies the conditions for avoiding slinky-type effects and, together with the choice of k_1, k_3, k_4, guarantees the stability of a platoon of vehicles. With this choice of gains the system is asymptotically stable and hence from (17) through (19) we see that $V_r \to 0, \delta \to 0$ for constant or slow changing V_l, S_0 and disturbance d. The importance of the extra term $k_3 V_r$ in (14) can be seen by examining (18). For $k_3 = 0$, the zeros of $\frac{\delta}{V_l}$ and $\frac{\delta}{S_0}$ are unstable, leading to possible undershoot in the transient response of δ.

The look-up table or equation (15) is developed by performing experiments. In these experiments a number of constant throttle input commands θ_0 taking values between θ_{min} and θ_{max} are used to calculate the corresponding vehicle speed V_0 at steady state. Since in our problem the desired speed is V_l we set $V_0 = V_l$ and calculate the corresponding throttle angle θ_0 by using the look-up table and interpolation where necessary.

The main equations of the PID controller are listed below:

$$\begin{aligned}
\theta_f &= f^{-1}(V_l) + k_1 V_r + k_2 \delta + \int_0^t (k_3 V_r + k_4 \delta) d\tau \\
k_1 &= (\lambda_0 + 2\zeta\omega_n - bk_2 h - a)/b \\
k_2 &= 0.2/b \\
k_3 &= (2\zeta\omega_n \lambda_0 + \omega_n^2 - bk_2 - h\lambda_0 \omega_n^2)/b \\
k_4 &= \lambda_0 \omega_n^2 / b.
\end{aligned} \tag{23}$$

The structure of the controller is shown in Figure 2.

In (23), the controller gains, k_1 to k_4, depend on h and the parameters a and b of the linearized dynamics of the throttle subsystem which in turn depend on the operating point (θ_0, V_0). These parameters may be calculated a priori at each operating point (θ_0, V_0) and listed in the look-up table for (θ_0, V_0). Consequently, k_1 to k_4 may be calculated as functions of $V_0 (= V_l)$. We refer to this scheme as the PID controller with gain scheduling. The gains, k_1 to k_4, may also be chosen according to some average or nominal values of a, b, and h and be invariant with respect to $V_0 (= V_l)$ and h. This leads to a PID controller with fixed gains. The use of a PID with fixed gains may be sufficient in many applications due to its inherent robustness properties with respect to modeling errors.

4.2 Adaptive Controller

The gain scheduling of the PID controller in Section 4.1 is based on a look-up table that is developed a ***priori*** by performing certain experiments. Instead of the look-up table one may use a parameter estimator or an adaptive law to update the gains of the PID controller on-line by processing the measured data. This leads to an adaptive control scheme referred to as adaptive controller. The advantage of the adaptive approach is that unpredictable

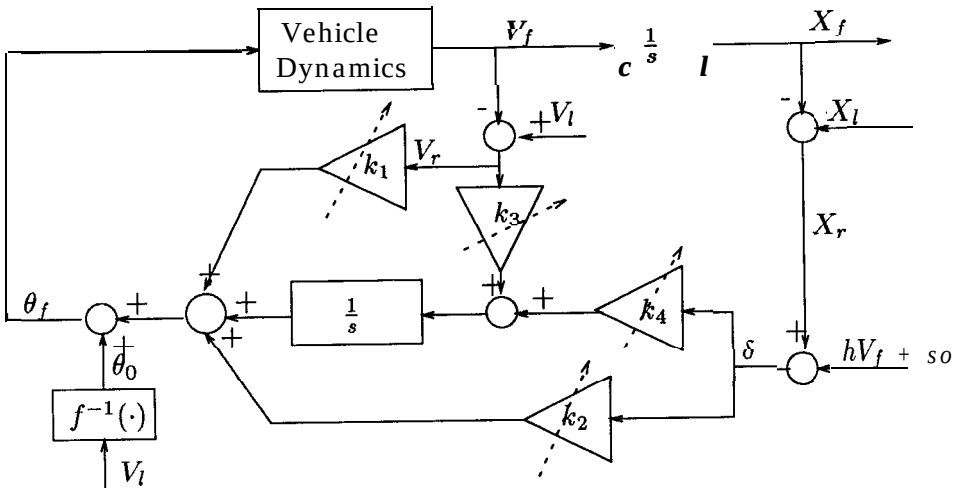

Figure *2:* PID throttle controller

changes in the values of a and ***b*** can be easily accommodated. In this subsection we design a direct adaptive controller as follows:

Form of the Control law:

Let us first assume that a, ***b*** and ***d*** are exactly known and derive the form of the control law that forms the basis for the adaptive control design. We consider the simple control law

$$\theta_f = \theta_0 + k_1 V_r + k_2 \delta + k_3 \tag{24}$$

where $V_r = V_l - V_f$. Substituting (24) into (13), we obtain the closed loop system.

$$\begin{aligned} \dot{X}_r &= V_l - V_f \\ \dot{V}_f &= -(a + bk_1)(V_f - V_l) + bk_2\delta + bk_3 + d \\ \delta &= X_r - hV_f - S_0 \\ V_r &= V_l - V_f \end{aligned} \tag{25}$$

which gives us

$$V_r = \frac{[s + (a + bk_2h)]s}{F(s)} V_l + \frac{bk_2 s}{F(s)} S_0 + \frac{s}{F(s)}(bk_3 + d) \tag{26}$$

$$\delta = \frac{[1 - h(a + bk_1)]s}{F(s)} V_l - \frac{(s + a + bk_1)s}{F(s)} S_0 - \frac{1 + hs}{F(s)}(bk_3 + d) \tag{27}$$

where

$$F(s) = s^2 + (a + bk_1 + bhk_2)s + bk_2.$$

The values of k_1, k_2 can now be chosen so that

$$s^2 + (a + bk_1 + bhk_2)s + bk_2 = s^2 + 2\zeta\omega_n s + \omega_n^2$$

where ω_n, ζ are chosen based on the performance requirements. The value of k_3 is chosen to eliminate the effect of the disturbance. Therefore we have that

$$\begin{aligned} k_1 &= (2\zeta\omega_n - h\omega_n^2 - a)/b \triangleq k_1^* \\ k_2 &= \omega_n^2/b \triangleq k_2^* \\ k_3 &= -d/b \triangleq k_3^*. \end{aligned} \tag{28}$$

With the above values of $k_1, k_2, kg,$ the closed-loop system becomes

$$\begin{aligned} V_r &= \frac{[s + (a + bk_2h)]s}{s^2 + 2\zeta\omega_n s + \omega_n^2} V_l + \frac{bk_2 s}{s^2 + 2\zeta\omega_n s + \omega_n^2} S_0 \\ \delta &= \frac{[1 - h(a + bk_1)]s}{s^2 + 2\zeta\omega_n s + \omega_n^2} V_l - \frac{(s + a + bk_1)s}{s^2 + 2\zeta\omega_n s + \omega_n^2} S_0 \end{aligned}$$

which show that for constant V_l, S_0, we have $V_r \to 0$, $\delta \to 0$ as $t \to \infty$ and hence the control design objective is achieved.

Adaptive Control law:

Since a, b, and d are unknown, the gains $k_i^* (i = 1, 2, 3)$, cannot be calculated from (28) and therefore (24) cannot be implemented with this choice of gains. Instead of (28), let us generate $k_i (i = 1, 2, 3)$ adaptively by estimating the desired gains $k_i^* (i = 1, 2, 3)$ as follows:

We first write the equation for V_f in (25) as

$$\begin{aligned} \dot{V}_f = {} & -a_m(V_f - V_l) + a_m k\delta + a_m(V_f - V_l) - a_m k\delta \\ & -(a + bk_1)(V_f - V_l) + bk_2\delta + bk_3 + d \\ = {} & -a_m V_f + a_m(V_l + k\delta) - (a + bk_1 - a_m)(V_f - V_l) \\ & +(bk_2 - a_m k)\delta + bk_3 + d \end{aligned} \tag{29}$$

where

$$a, = a + bk_1^*, \quad k = bk_2^*/(a + bk_1^*). \tag{30}$$

Using (28),(29) and (30), we have that

$$\dot{V}_f = -a_m V_f + a_m(V_l + k\delta) + b(k_1 - k_1^*)V_r + b(k_2 - k_2^*)\delta + b(k_3 - k_3^*)$$

i.e.

$$V_f = \frac{a_m}{s + a_m}[V_l + k\delta] + \frac{b}{s + a_m}[\tilde{k}_1 V_r + \tilde{k}_2\delta + \tilde{k}_3] \tag{31}$$

where $\tilde{k}_i = k_i - k_i^* (i = 1, 2, 3)$ and s is taken as the differential operator. Making $k_i \to k_i^*$, $i = 1, 2, 3$, is equivalent to making $V_f \to \frac{a_m}{s+a_m}[V_l + k\delta]$ in some sense. Thus let us consider the error e_1 which is defined as

$$e_1 \triangleq \boldsymbol{Vj} - \frac{a_m}{s + a_m}[V_l + k\delta]. \tag{32}$$

From (31) and (32) we have that

$$e_1 = \frac{b}{s + a_m}[\tilde{k}_1 V_r + \tilde{k}_2 \delta + \tilde{k}_3]. \tag{33}$$

We now define a new error signal

$$\epsilon \triangleq e_1 - \frac{\lambda}{s + a_m}\epsilon m^2 \tag{34}$$

which together with (33) implies that

$$\dot{\epsilon} = -a_m \epsilon + b\tilde{k}_1 V_r + \boldsymbol{b\&S} + b\tilde{k}_3 - \lambda \epsilon m^2 \tag{35}$$

where $m^2 = \delta^2 + V_r^2$. The signal ϵ is the so called normalized estimation error defined in [15]. From this definition we see that at steady state, ϵ is roughly equal to $a_m e_1/(a_m + \lambda m^2)$. Thus if $\boldsymbol{m} >> 1$, then $\epsilon \ll e_1$ and if m << 1 then $\epsilon \approx e_1$. As seen below, we will use ϵ instead of e_1 to update k_1, k_2, and $\boldsymbol{kg}$. The reason is that ϵ is a normalized version of e_1 and therefore with ϵ, the adjustment of k_i $(i = 1, 2, 3)$ is slow relative to the possible rapid changes in e_1. This slow speed of adaptation helps robustness by keeping the bandwidth of the controller in the low frequency range. The adaptive law is derived by using the Lyapunov-like function

$$L_y = \frac{\epsilon^2}{2} + b\frac{\tilde{k}_1^2}{2\gamma_1} + b\frac{\tilde{k}_2^2}{2\gamma_2} + b\frac{\tilde{k}_3^2}{2\gamma_3} \tag{36}$$

where $\gamma_i > 0$ and $\boldsymbol{b}$, even though unknown, is always positive according to our simulations on the validated nonlinear model. The time derivative of L_y along the solution of (35) is

$$\dot{L}_y = -a_m \epsilon^2 - \lambda \epsilon^2 m^2 + \epsilon b \tilde{k}_1 V_r + \epsilon b \tilde{k}_2 \delta + \epsilon b \tilde{k}_3 + \sum_{i=1}^{3} b\frac{\tilde{k}_i}{\gamma_i}\dot{\tilde{k}}. \tag{37}$$

Choosing

$$\begin{aligned} \dot{k}_1 &= -\gamma_1 \epsilon V_r \\ \dot{k}_2 &= -\gamma_2 \delta \epsilon \\ \dot{k}_3 &= -\gamma_3 \epsilon \end{aligned} \tag{38}$$

we have that

$$\dot{L}_y = -a_m \epsilon^2 - \lambda \epsilon^2 m^2 \tag{39}$$

which implies that $e_1, \epsilon \in L_2 \cap L_\infty$ and hence $\tilde{k}_i \in L_\infty (i = 1, 2, 3)$. Following the approach of [15] we can further show that $e_1, \epsilon \to 0$ and $V_f \to V_l$ and $\delta \to 0$ for constant V_l.

For robustness the adaptive laws for $k_i (i = 1, 2, 3)$ in (38) can be modified to

$$\dot{k}_i = \begin{cases} 0 & \text{if } k_i \geq k_{u_i} \text{ and } g_i > 0 \\ 0 & \text{if } k_i \leq k_{\ell_i} \text{ and } g_i < 0 \\ g_i & \text{otherwise} \end{cases} \tag{40}$$

where k_{u_i}, k_{ℓ_i} are upper and lower bounds for k_i respectively and $g_1 = -\sigma_1(k_1 - \mathbf{km}) - \gamma_1 V_r \epsilon$, $g_2 = -\sigma_2(k_2 - k_{20}) - \gamma_2 \delta \epsilon$, and $g_3 = -\gamma_3 \epsilon$ where $\sigma_i > 0$ $(i = 1, 2, 3)$ are small design constants and k_{i0} is the initial estimate of k_i^* for $i = 1, 2$. The modified adaptive law (40) guarantees that $k_{\ell_i} \leq k_i(t) \leq k_{u_i} \quad \forall t > 0$ provided $\mathbf{k;(O)}$ satisfies $k_{\ell_i} \leq \mathbf{k;(O)} \leq k_{u_i}$. By constraining the gains k_i within certain bounds we avoid the generation of high gain feedback that may cause instability or deterioration of performance due to excessive excitation of the unmodeled dynamics [15]. The modification (40) does not alter the stability properties established for the adaptive law (38) without modification [15].

In the above design, we first choose ζ, ω_n and then use (28), (30) to determine $\mathbf{a,}$ and $\mathbf{k}$. We can also choose $\mathbf{a,}$ and $\mathbf{k}$ directly.

We summarize the main equations of the above adaptive controller below:

$$\begin{aligned} \theta_f &= f^{-1}(V_l) + k_1 V_r + k_2 \delta + k_3 \\ \dot{k}_i &= \begin{cases} \mathbf{0} & \text{if } k_i \geq k_{u_i} \text{ and } g_i > 0 \\ 0 & \text{if } k_i \leq k_{\ell_i} \text{and } g_i < 0 \\ g_i(\epsilon, V_f, \delta) & \text{otherwise} \end{cases} \\ \epsilon &= e_1 - \frac{1}{s + a_m} \lambda \epsilon m^2 \\ e_1 &= V_f - \frac{a_m}{s + a_m}[V_l + k\delta] \\ m^2 &= \delta^2 + V_r^2 \end{aligned} \tag{41}$$

where $i = 1, 2, 3$, $g_1 = -\sigma_1(k_1 - k_{10}) - \gamma_1 \epsilon V_r$, $g_2 = -\sigma_2(k_2 - k_{20}) - \gamma_2 \epsilon \delta$, $g_3 = -\gamma_3 \epsilon$. The structure of the adaptive controller is shown in Figure 3.

4.3 Modified Control Schemes

The control schemes of the previous subsections will guarantee that $V_r, \delta \to \mathbf{0}$ for any constant leading vehicle speed V_l. They cannot guarantee however that constraints Cl, C2 are met during transients. For example if V_l changes rapidly at a particular point of time, it may create a large error, i.e., large V_r, δ, which in turn may cause large throttle angle and acceleration, violating constraints Cl, C2. Another case is when the following vehicle switches following from one vehicle to another due to lane change etc. Such change may introduce a large initial position error $|\delta(0)|$ and speed error $|V_r(0)|$ leading to high acceleration/deceleration that may violate constraints Cl, C2. In order to meet constraint

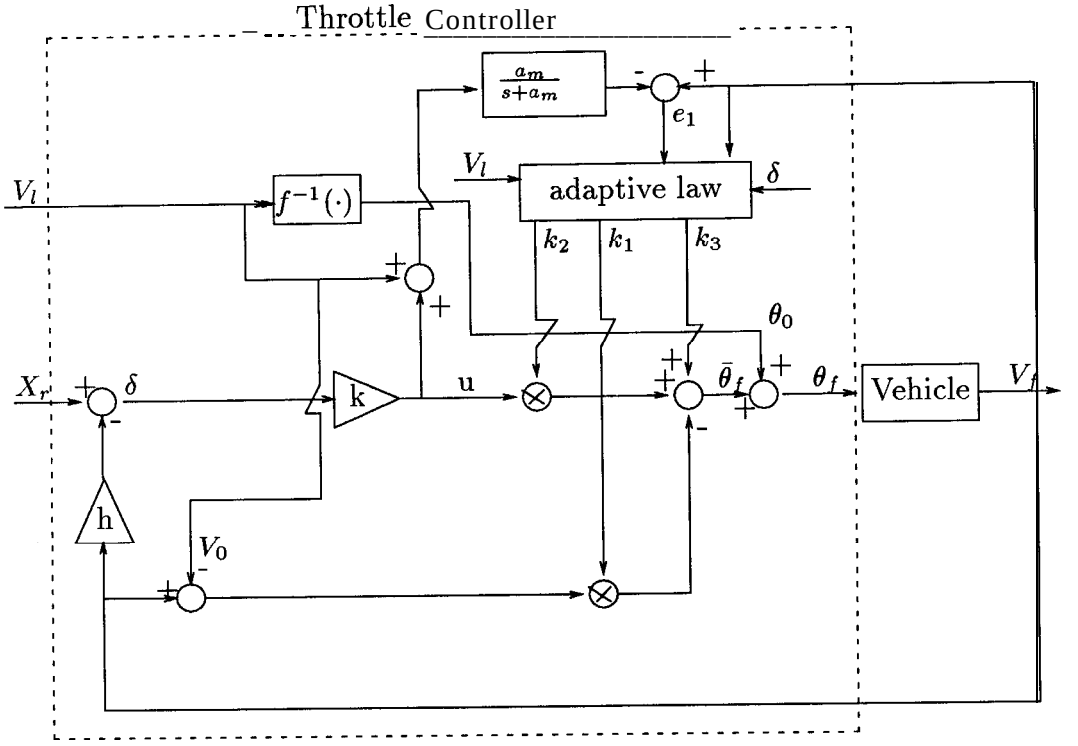

Figure 3: Adaptive controller

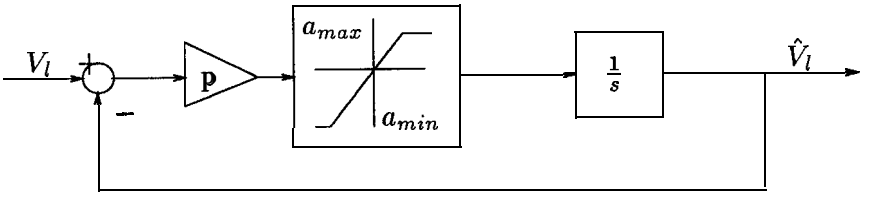

Figure 4: Acceleration limiter

Cl and protect the following vehicle from responding to erratic behavior of the leading vehicle we pass V_l through an acceleration limiter shown in Figure 4 where p is some positive constant. The output of the acceleration limiter is $\hat{V}_l$. Instead of following V_l, ***we*** try to follow $\hat{V}_l$. The acceleration limiter eliminates any erratic or sudden changes in V_l during transients and presents a smoother trajectory to the follower. It also serves as a low pass filter for V_l. At steady state, $\hat{V}_l$ approaches V_l and therefore by following V_l we reach V_l eventually in a smooth way.

The effect of large initial error $|\delta(0)|$ is taken care of by introducing a saturation element sat(S) which is defined as

$$\text{sat(b)} = \begin{cases} e_{max} \text{ if } \delta > e_{max} \\ e_{min} \text{ if } \delta < e_{min} \\ \delta \quad \text{otherwise} \end{cases} \tag{42}$$

and limits the measurements seen by the controller to be within e_{max} and e_{min}. Note that, since negative position error means short intervehicle spacing, thus $|e_{min}|$ is much larger than e_{max}.

Using these two modifications, the control schemes of the previous sections are modified as shown below:

1. PID Controller with Fixed Gain

$$\theta_f = f^{-1}(\hat{V}_l) + k_1(\hat{V}_l - V_f) + k_2 \text{ sat(S)} + \int_{00}^{t} [k_3(\hat{V}_l - V_f) + k_4 \text{ sat}(\delta)]d\tau \tag{43}$$

2. PID Controller with Gain Scheduling

$$\begin{aligned} \theta_f &= f^{-1}(\hat{V}_l) + k_1(\hat{V}_l - V_f) + k_2 \text{ sat}(\delta) + \int_0^t [k_3(\hat{V}_l - V_f) + k_4 \text{ sat}(\delta)]d\tau \\ k_1 &= (\lambda_0 + 2\zeta\omega_n - bk_2h - a)/b \\ k_2 &= \textbf{0.2/b} \\ k_3 &= (2\zeta\omega_n\lambda_0 + \omega_n^2 - bk_2 - h\lambda_0\omega_n^2)/b \\ k_4 &= \lambda_0\omega_n^2/b \end{aligned} \tag{44}$$

3. Adaptive Controller

$$\begin{aligned} \theta_f &= f^{-1}(\hat{V}_l) + k_1(\hat{V}_l - V_f) + k_2 \, sat(S) + k_3 \\ \dot{k}_i &= \begin{cases} 0 & \text{if } k_i \geq k_{u_i} \text{ and } g_i > 0 \\ 0 & \text{if } k_i \leq k_{\ell_i} \text{and } g_i < 0 \\ g_i(\epsilon, V_f, \delta) & \text{otherwise} \end{cases} \\ \epsilon &= e_1 - \frac{1}{s + a_m}\lambda\epsilon m^2 \end{aligned} \tag{45}$$

$$
\begin{aligned}
e_1 &= V_f - \frac{a_m}{s + a_m}(\hat{V}_l + k\delta) \\
m^2 &= (\text{sat}(\delta))^2 + (V_f - \hat{V}_l)^2
\end{aligned}
$$

where $i = 1, 2, 3$, $g_1 = -\sigma_1(k_1 - k_{10}) + \gamma_1\epsilon(V_f - \hat{V}_l)$, $g_2 = -\sigma_2(k_2 - k_{20}) - \gamma_2\epsilon\ \text{sat}(\delta)$, $g_3 = -\gamma_3\epsilon$.

In the above modified throttle controllers, the $\hat{V}_l$ trajectory is defined as

$$
\dot{\hat{V}}_l = \begin{cases} a_{max} & \text{if } p(V_l - \hat{V}_l) \geq a_{max} \\ p(V_l - \hat{V}_l) & \text{if } a_{min} < p(V_l - \hat{V}_l) < a_{max} \\ a_{min} & \text{if } p(V_l - \hat{V}_l) \leq a_{min} \end{cases} \tag{46}
$$

The low pass character of the throttle actuator together with the acceleration limiter and the saturation function introduced by the controller will also lead to a smooth throttle angle response and help reduce the amount of jerk. In order to attenuate the effect of sensor noise in the measurements and further reduce jerk, we use the following low pass filter

$$
\frac{c_0}{s + c_0} \tag{47}
$$

to filter X,., V_l, and V_f, where c_0 is some constant chosen based on the sampling rate and noise level. For simplicity, these filters are not included in the equations for our controllers.

5 Brake Control Design and Analysis

Automatic vehicle following may be achieved by using the throttle controller in most cases where the required torque for acceleration or deceleration can be generated by the engine alone. When the leading vehicle is decelerating fast or during downhill vehicle following situations, the engine torque may not be sufficient to achieve vehicle following without using the brake. In this section we assume that the following vehicle is in a situation that the brake has to be applied and design a controller to control the brake line pressure.

The dynamic equations related to the brake torque developed in Section 2 are:

$$
\begin{aligned}
\dot{X}_r &= V_l - V_f \\
\dot{V}_f &= \tfrac{1}{M}(-c_1 T_b - f_0 - c_2 V_f - c_3 V_f^2) \\
\delta &= X_{,.} - hV_f - So \\
V_r &= V_l - V_f
\end{aligned} \tag{48}
$$

Since what we actually control in the brake system is the brake line pressure defined as P_r which is approximately proportional to the brake torque, we rewrite (48) as

$$
\begin{aligned}
\dot{X}_r &= V_l - V_f \\
\dot{V}_f &= \tfrac{1}{M}(-c_4 P_r - f_0 - c_2 V_f - c_3 V_f^2) \\
\delta &= X_r - hV_f - S_0 \\
V_r &= V_l - V_f
\end{aligned} \tag{49}
$$

where P_r is the control input and c_4 is a known constant. We then use feedback linearization to transform (49) into the linear system

$$\begin{aligned} \dot{X}_r &= V_l - V_f \\ \dot{V}_f &= u \\ \delta &= X_r - hV_f - So \\ V_r &= V_l - V_f \end{aligned} \tag{50}$$

where

$$u = \frac{1}{M}(-c_4 P_r - f_0 - c_2 V_f - c_3 V_f^2). \tag{51}$$

We can now use techniques from linear system theory to choose the desired input u that stabilizes the system given by (50) and forces δ, V_r to converge to zero. From the desired input u we calculate the desired line pressure P_r by solving for P_r in (51).

We start by proposing the feedback control

$$u = k_5 V_r + k_6 \delta \tag{52}$$

where k_5 and k_6 are design parameters. Substituting (52) into (50), we have

$$\begin{aligned} \dot{X}_r &= V_l - V_f \\ \dot{V}_f &= k_5 V_r + k_6 \delta \\ \delta &= X_r - hV_f - So \\ V_r &= V_l - V_f. \end{aligned} \tag{53}$$

Hence

$$V_r = \frac{(s + k_6 h)s}{\Delta_b(s)} V_l + \frac{k_6 s}{\Delta_b(s)} S_0 \tag{54}$$

$$\delta = \frac{(1 - k_5 h)s}{\Delta_b(s)} V_l - \frac{(s + k_5)s}{\Delta_b(s)} S_0 \tag{55}$$

where

$$\Delta_b(s) = s^2 + (k_5 + k_6 h)s + k_6. \tag{56}$$

It is clear from equations (54)—(56) that the system is stable for any finite k_5 and $k_6 > 0$. Furthermore, for V_l = constant we have $V_r, \delta \to 0$ as $t \to \infty$. Also when $\dot{V}_l = a_l$ = constant, equation (54) implies that at steady state $V_r = ha_l$ which in turn implies that $\dot{V}_f = a_l$ at steady state.

Even though the system is stable for any positive values of k_5, ***kg,*** the specific choice of ***kg,*** k_6 will affect the performance of the system. From (55) it follows that if we choose k_5 such that $1 - k_5 h = 0$ then δ will not be affected by $\dot{V}_l$. Moreover, in order to avoid overshoot in V_r and δ with constant $\dot{V}_l$, we should choose ***kg,*** k_6 such that $\Delta_b(s) = 0$ has two real negative roots. This choice of ***kg,*** k_6 will in turn help prevent oscillations in the braking

force that may signal switching of the brake between the on and off positions. Another consideration in the choice of k_5, k_6 is the bandwidth of the controller which should be small relative to that of the brake actuator and sensor dynamics. In our design we assume that h assumes values between ***0.4*** to 1.5 seconds and choose $k_5 = 1$ and $k_6 = 0.25$ that lead to the roots $r_1 \in$ [-1.15, -0.7791 , $r_2 \in$ [-0.321, -0.2161 for $\Delta_b(s) = 0$. Given the above choice for ***kg,*** k_6 the desired line pressure is given by

$$P_r = \frac{-1}{c_4}[M(k_5 V_r + k_6 \delta) + f_0 + c_2 V_f + c_3 V_f^2]. \tag{57}$$

In the above design, we did not take into account constraint **Cl.** Noting that $k_5 V_r + k_6 \delta$ is the desired deceleration of the following vehicle, in order to satisfy constraint **Cl,** we put a saturation on $k_5 V_r + k_6 \delta$, leading to the modified expression for the desired line pressure:

$$P_r = \begin{cases} 0 & \text{if } -M(k_5 V_r + k_6 \delta) < f_0 + c_2 V_f + c_3 V_f^2 \\ \frac{-1}{c_4}(M\, a_{min} + f_0 + c_2 V_f + c_3 V_f^2) & \text{if } k_5 V_r + k_6 \delta < a_{min} \\ \frac{-1}{c_4}[M(k_5 V_r + k_6 \delta) + f_0 + c_2 V_f + c_3 V_f^2] & \text{otherwise} \end{cases} \tag{58}$$

The above desired P_r may have a discontinuity at the time the brake controller is turned on. Since the brake actuator acts as a low pass filter, the output of the actuator is smooth, leading to a smooth braking force and therefore any discontinuities in ***P,.*** will not lead to rough braking.

Remark In contrast to the throttle controller design, the brake controller has no integral action for rejecting disturbances. The reason is that the brake is applied only for a short time and any position error that may arise during braking due to disturbances will be taken care of by the throttle controller.

6 Logic Switch for Throttle and Brake Controllers

In the previous sections we designed controllers for the throttle and brake subsystems. Since in our approach the throttle and brake controllers are not allowed to act together at any given time, we need to develop the appropriate logic that dictates the switching procedure from the throttle controller to the brake controller and vice versa. Our approach and logic ***is*** based on the way that a good driver uses the brake and accelerator pedals. For example a good driver never uses both pedals at the same time, and he uses the brake only when he wants to achieve rapid and large deceleration and avoids frequent switchings from one pedal to another. Using the intuition of an ideal driver we develop the logic in a way that constraints **Cl, C2** are satisfied. The switching logic is based on the following situations:

Situation 1: X,. $< X_{min}$ and $V_f > V_1$

This situation arises when the following vehicle is at high speed (i.e. $V_f > V_1$) and relatively close to the leading vehicle (i.e. $X_r < X_{min}$). The constants X_{min}, V_1 are design variables that are chosen according to the braking capabilities of the vehicle. In our design

X_{min} = 6 meters and $V_1 = 13.4$ m/s. When this situation arises, the brake controller is switched on and remains on until (V_r, P_{er}), where P_{er} is defined as the percentage position error, i.e., $P_{er} \triangleq \frac{6}{hV_f + S_0} \times 100$, is inside the shaded region shown in Figure 5, at which time the brake controller is switched off. When the brake controller is switched off, it remains switched off inside and outside the shaded region shown in Figure 5 until the situation where $X_r < X_{min}$ and $V_f > V_1$ come up again.

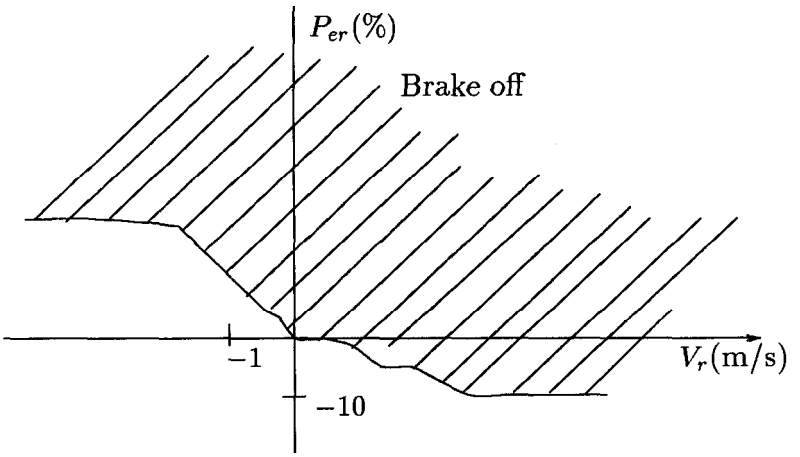

Figure 5: Logic switch for brake off when X,. < X_{min} and $V_f > V_1$

Situation 2: $X_r > X_{max}$

In this situation the relative distance is large enough and no braking is necessary. Therefore the brake controller is off independent of any other condition. In our case the design constant X_{max} is chosen to be equal to 40 meters.

Situation 3: $X_{min} \leq$ X,. $\leq X_{max}$, or $X_r < X_{min}$ and $V_f \leq V_1$

In this situation the switching from brake to throttle and vice versa is dictated by the values of V_r, P_{er} and the value of throttle angle command θ_f as shown in Figure 6. The plane shown in Figure 6 is divided into three regions. When (V_r, P_{er}) is in region 1 and the throttle angle command $\theta_f \leq \theta_{min}$, where θ_{min} is the minimum throttle angle for idle engine speed, the brake controller is switched on and remains switched on until (V_r, P_{er}) reaches region 2 where the brake controller is switched off. Region 3 can be crossed from each direction, i.e., from brake on in region 1 to brake off in region 2 and vice versa and therefore acts as a neutral region where the brake is off or on depending on the region we start from. This neutral region introduces a hysteresis in the switching process that eliminates the possibility of oscillating between throttle and brake with high frequency.

Remarks

- When the brake controller is turned on, the throttle controller is turned off and the

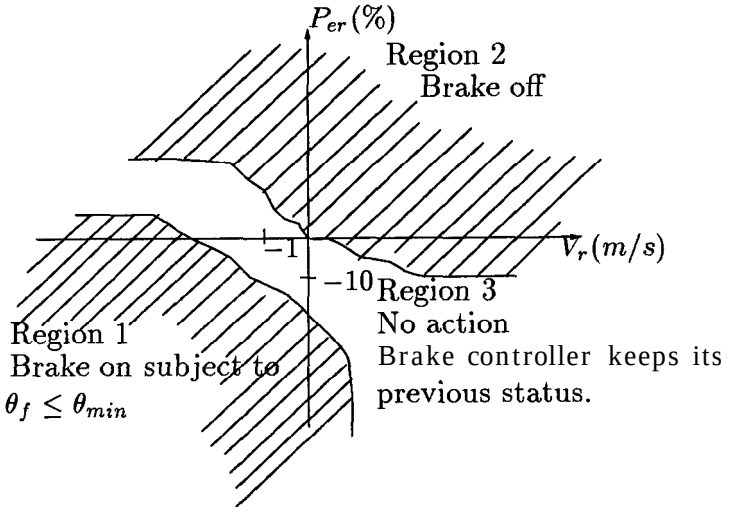

Figure 6: Logic switch for brake on and off when $X_{min} \leq X_r \leq X_{max}$, or X,. < X_{min} and $V_f \leq V_1$

throttle command is set to the minimum value. Similarly when the brake controller is turned off, the throttle one is turned on.

- The position error δ is used in both throttle and brake controllers, but the percentage of the position error P_{er} is used in the switching logic. The reason for this is that P_{er} is a better measure of the closeness of the two vehicles.
- Figures 5 and 6 only show the corresponding regions approximately. The non-smoothness of the boundary of the regions is due to the software used to draw these figures.

7 Platoon Stability Analysis

The emphasis of the previous sections was on the stability and response of a vehicle that follows a leading one automatically. When a number of vehicles follow each other in the same manner, we have a platoon of vehicles which has its own dynamics and response. In this case, the stability and good response of each individual vehicle does not imply stability and good response for the platoon [16]. A phenomenon known as slinky-type effect [3] or "accordion" effect where a small disturbance in position, velocity, or acceleration may be amplified from one vehicle to another within the platoon may easily take place. The platoon is considered to be stable if it is free from slinky-type effects. Providing this type of stability within a platoon is extremely important since it permits the platoon to recover from disturbances and ensures that tracking errors are attenuated with increasing distance from the disturbance source.

In the following, we will show that, with the proper choice of the controller parameters,

platoon stability can be assured by the proposed PID controller with gain scheduling and adaptive controller.

Analysis of platoon dynamics Consider vehicles following each other in a single lane with no passing, forming a platoon as shown in Figure (7). In this platoon, there is no communication between vehicles and each vehicle is a leading vehicle for the vehicle immediately behind it. We assume that, in the platoon, all the vehicles except for the platoon leader are using throttle control only and that throttle controllers in all vehicles are the same. The reasons for this assumption are as follows: (a) with the brake controller, the platoon dynamic analysis is very difficult since the use of brake controller involves the switching logic which is nonlinear, (b) in the platoon analysis, we focus on the propagation of small deviations through the platoon during normal operation where no braking is needed.

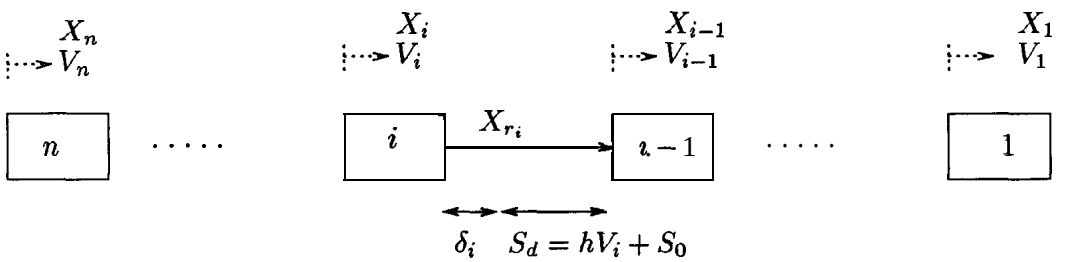

Figure 7: Platoon of Vehicles

As shown in Figure (7), δ_i is the deviation of the i-th vehicle from the desired spacing $S_d = hV_i + S_o$, i.e.,

$$\delta_i = X_{r_i} - hV_i - S_o \tag{59}$$

where X_{r_i} are the relative distance between the front bumper of the i-th vehicle and rear bumper of the $(i-1)$-th vehicle, X_i and V_i are the position and speed of the i-th vehicle, respectively. We assume that all the vehicles are operating around some constant speed (operating point) V_0 and the deviations δ_i and $V_{r_i} \triangleq V_{i-1} - V_i$ are small. This assumption enables us to operate within the acceleration limit and position error saturation limit introduced in subsection 4.3. Because the constant S_0 and disturbance $\boldsymbol{d}$ do not affect the platoon dynamics, we ignore them in our analysis.

PID controller with gain scheduling

From equations (17) — (20) we can find the transfer function between δ_i and δ_{i-1} as follows:

$$G_1(s) \triangleq \frac{\delta_i}{\delta_{i-1}} = \frac{(\lambda_0 + 2\zeta\omega_n - hk_2b)s^2 + (2\zeta\omega_n\lambda_0 + \omega_n^2 - h\lambda_0\omega_n^2)s + \lambda_0\omega_n}{(s+\lambda_0)(s^2 + 2\zeta\omega_n s + \omega_n^2)} \tag{60}$$

where λ_0, ω_n, and ζ are related to k_1, k_2, k_3, k_4 through (21) and (22). We can also show that

$$\frac{V_{r_i}}{V_{r_{i-1}}} = \frac{\delta_i}{\delta_{i-1}} = G_1(s) \tag{61}$$

Based on the fact that if $y = G(s)u$, then $||y||_2 \leq \sup_\omega |G(j\omega)| ||u||_2$, the condition for platoon stability is

$$|G_1(j\omega)| < 1, \quad \forall\omega > 0. \tag{62}$$

After tedious calculations we find that a set of sufficient conditions to satisfy (62) is

$$\begin{aligned} 2\zeta\omega_n\lambda_0 + \omega_n^2 &> h\lambda_0\omega_n^2/2 + bk_2 \\ \lambda_0 + 2\zeta\omega_n &> \frac{2\zeta\omega_n\lambda_0 + \omega_n^2}{hbk_2} + \frac{hbk_2}{2} \end{aligned} \tag{63}$$

Thus, to assure platoon stability, we can choose $\lambda_0, \zeta, \omega_n$ and k_2 such that (63) is satisfied and then calculate k_1, k_3, k_4 based on (21). To simplify this choice, we can choose $bk_2 = 0.2$.

It is interesting to investigate the case when constant spacing policy is adopted. In this case $h = 0$, and the inequality (62) is equivalent to

$$\omega^2 - 2(2\zeta\omega_n\lambda_0 + \omega_n^2) > 0, \quad \forall\omega > 0. \tag{64}$$

Since ζ, ω_n, and λ_0 are positive, (64) can not be satisfied. In other words, platoon stability can not be achieved if constant spacing policy is adopted by the proposed PID controller with gain scheduling.

Adaptive controller

In section 4.2, we have shown that the proposed adaptive controller will drive $e_{1_i}(t)$ which is defined as

$$e_{1_i} \triangleq V_i - \frac{a_m}{s+a_m}(V_{i-1} + k\delta_i) = \frac{b}{s+a_m}[\tilde{k}_1 V_{r_i} + \tilde{k}_2\delta_i + \tilde{k}_3]$$

to zero for constant V_{i-1}. Now we further assume that the adaptation speed of the controller is fast enough so that we can approximate V_i by $\frac{a_m}{s+a_m}(V_{i-1} + k\delta_i)$. That is

$$V_i \approx \frac{a_m}{s+a_m}(V_{i-1} + k\delta_i)$$

or

$$\dot{V}_i \approx a_m(V_{i-1} - V_i) + a_m k\delta_i. \tag{65}$$

Differentiating (59) twice and using (65), we obtain

$$\begin{aligned} \ddot{\delta}_i &= \dot{V}_{i-1} - \dot{V}_i - h\ddot{V}_i \\ &= a_m(V_{i-2} - V_{i-1}) + a_m k\delta_{i-1}) - [a_m(V_{i-1} - V_i) + a_m k\delta_i)] \\ &\quad -h[a_m(\dot{V}_{i-1} - \dot{V}_i) + a_m k\dot{\delta}_i)] \end{aligned}$$

The relationship between δ_i and δ_{i-1} with zero initial conditions can be derived as:

$$G_1(s) \triangleq \frac{\delta_i(s)}{\delta_{i-1}(s)} = \frac{a_m s + a_m k}{s^2 + (ha_m k + a_m)s + a_m k} \tag{66}$$

It can also be shown that

$$\frac{V_{r_i}(s)}{V_{r_{i-1}}(s)} = G_1(s). \tag{67}$$

After some calculation, we find that inequality (62) is equivalent to

$$\omega^2 + [a_m^2 k^2 h^2 + 2a_m^2 kh - 2a_m k] > 0, \quad \forall w > 0 \tag{68}$$

The above inequality can be satisfied if and only if

$$a_m^2 h^2 k^2 + 2a_m^2 hk - 2a_m k > 0$$

which is equivalent to

$$k[a_m h^2 k + 2a_m h - 23 > 0$$

Since k is positive to assure each root of G_1 (s) on the open left s-plane, the platoon stability can be achieved by the proposed adaptive controller if we choose

$$k > \frac{2}{a_m h^2}(1 - a_m h). \tag{69}$$

Remark If $h = 0$ which corresponds to constant spacing policy, the inequality (68) can be rewritten as:

$$\omega^2 - 2a_m k > 0, \quad VW > 0$$

Since k, a, > 0, the above inequality cannot be satisfied for $\omega^2 < 2a_m k$. Hence, platoon stability cannot be achieved by the proposed adaptive control law if constant spacing policy is adopted. In this case, vehicle to vehicle communication is needed in order to guarantee platoon stability [3].

8 Simulation and Experimental Results

In order to test the controllers designed in Sections 4 through 7, we apply them to the validated original nonlinear vehicle model and perform a series of simulations. The throttle controllers simulated are: a PID throttle controller with fixed gain, a PID throttle controller with gain scheduling and an adaptive throttle controller. All three throttle controllers are integrated with the same brake controller and switching logic designed in Sections 5 and 6. For convenience, we will refer to the integrated controller consisting of the adaptive throttle controller, the brake controller, and the switching logic as the adaptive controller. We follow a similar notation for the fixed gain PID and the PID controller with gain scheduling.

In these simulations, we include the low pass filters (47) for X,., V_l, V_f. The parameters of the controllers are chosen as follows:

Fixed gain PID throttle controller:

$k_1 = 14.5$, $k_2 = 3$, $kg = 0.23$, $k_4 = 0.23$, $e_{max} = 3$ meters, $e_{min} = -100$ meters;

PID throttle controller with gain scheduling:

$\omega_n = 0.1$, $\zeta = 1$, $\lambda_0 = 1.2$, $e_{max} = 3$ meters, $e_{min} = -100$ meters;

The gains k_1, k_2, kg, k_4 are updating using (23) with $h = 1$.

Adaptive controller

$a_m = 0.8$, $\lambda = 0.05$, $k = 0.9$
$\gamma_1 = 1$, $\gamma_2 = 0.4$, $\gamma_3 = 0.67$
$\sigma_1 = 0.025$, $\sigma_2 = 0.005$
$k_{u_1} = 16$, $k_{l_1} = 2$, $k_{10} = 8$
$k_{u_2} = 10$, $k_{l_2} = 0.1$, $k_{20} = 4$
$k_{u_3} = 70$, $k_{l_3} = -70$
$e_{max} = 1.8$ meters, $e_{min} = -100$ meters

Acceleration constraints:

$$a_{max} = 0.1g, a_{min} = -0.2g.$$

0 t her parameters:

p = 10, $c_0 = 10$.

For this choice of parameter, it can be checked that the platoon stability conditions for the PID controller with gain scheduling and the adaptive controller are satisfied for h around 1 second.

The simulation results for two vehicle following are shown in Figures 8(a) — (g) among which Figure 8(a) shows the speed profile of the leading and following vehicles for the three different controllers.

At $t = 0$, both leading vehicle and following vehicle have zero speed and the following vehicle is at the desired position. From $t = 0$ to $t = 60$ second, the leading vehicle's speed is first increased to 15.6m/s with an acceleration of $0.0685g$ and then is kept at 15.6m/s. It is clear from these figures that, in this time period, good velocity tracking is achieved by the PID controller with gain scheduling and the adaptive controller, the position error is small, and the acceleration approximately satisfies the constraints. The fixed gain PID controller causes some oscillation in the acceleration response and throttle command (see Figures 8(c) and (g)), which means that under the fixed gain PID controller at low speed, the driver and passengers will not feel as comfortable as under the PID controller with gain scheduling and the adaptive controller.

From $t = 60$ to $t = 140$ second, the leading vehicle's speed is first increased from 15.6m/s to 24.6m/s with an acceleration of $0.285g$ and then maintained at 24.6m/s. Due to the acceleration limiter we put on the following vehicle, a large positive error appears during the transient. However, when the leading vehicle is at constant speed, the following vehicle catches up fairly soon. As we expected, the acceleration of the following vehicle with each controller satisfies the constraints even when the leading vehicle acceleration is well above the allowable limits.

From $t = 140$ to $t = 200$ second, we test the performance of the controllers at high speed with smooth leading vehicle speed trajectory. This test is similar to the test for the time period of [0, 60] second. It is easy to see that all the three controllers have similar good performance in position, speed and acceleration at high speed.

Starting from $t = 200$ second, we reduce the time headway from $h = 1$ second to $h = 0.8$ seconds (see Fig. S(d)). This implies that we want to have a smaller intervehicle spacing. From Fig. 8(a) we see that the following vehicle first increases its speed in order to create a smaller intervehicle spacing and then speeds down to match the leading vehicle speed.

Starting from $t = 250$ second, the leading vehicle speed is decreased from 33.5m/s to 22.3m/s with a deceleration of 0.19g. Since such deceleration cannot be achieved by using engine torque only, the brake controller becomes active. The desired brake line pressure is shown in Fig. 8(e). From Fig. 8(e) we see that this is the only time we apply the brake and there are no oscillations in the brake line pressure. Because of the time delay due to brake actuator and logic switch, there is about 5 meter negative position error (which means short intervehicle spacing) for each controller. If there were vehicle to vehicle communication, we could send the brake action to the following vehicle, reduce the time delay due to the switching logic and therefore reduce the position error.

At time $t = 310$ second, we introduce a large disturbance which is shown in Fig. 8(f). This disturbance is approximately equal to the force which appears when the vehicle goes up a hill with a 5.5 degree slope. It is seen that each of the controllers rejects the effect of the disturbance.

We demonstrate the platoon stability by simulating a five vehicle platoon under the

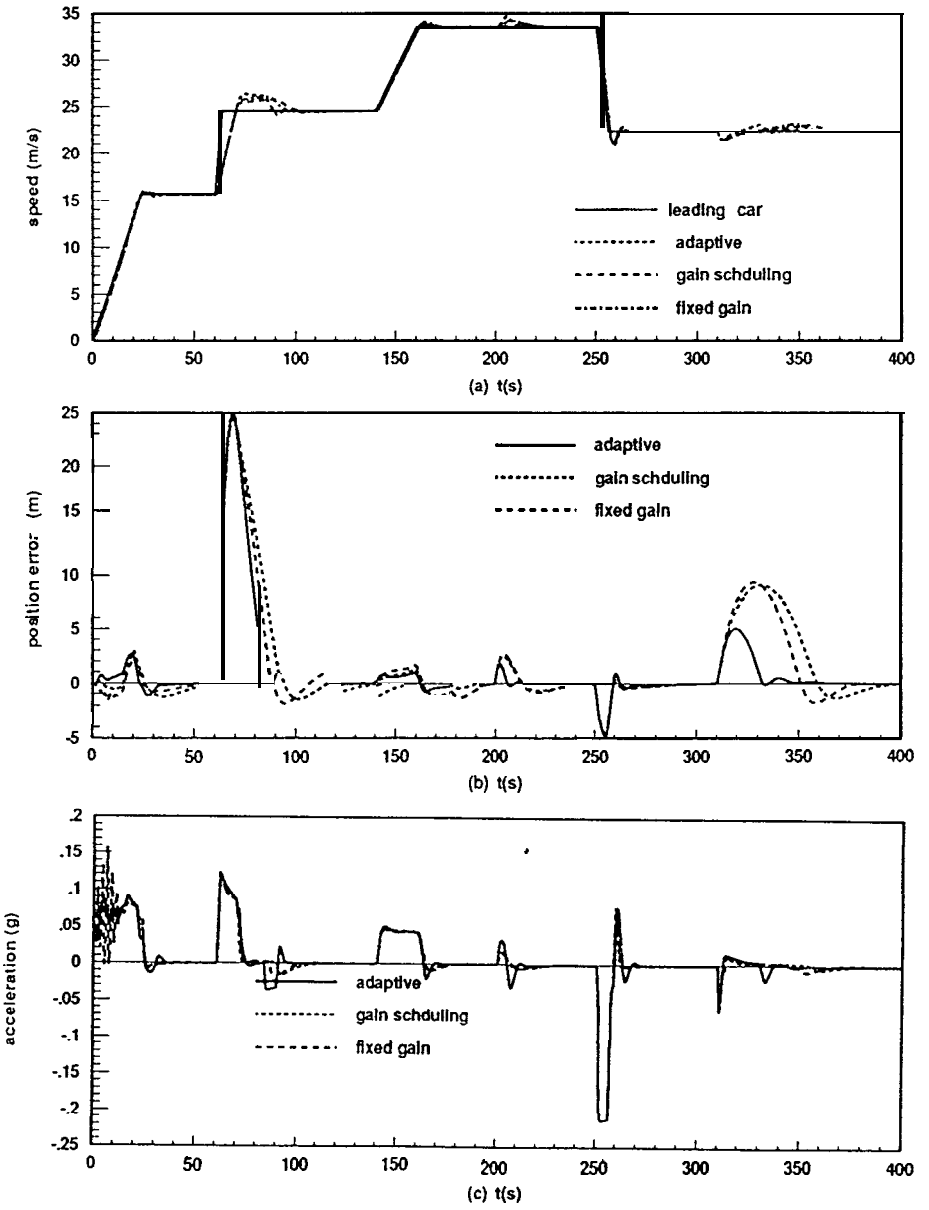

Figure 8: (a-c) Simulation results of three controllers

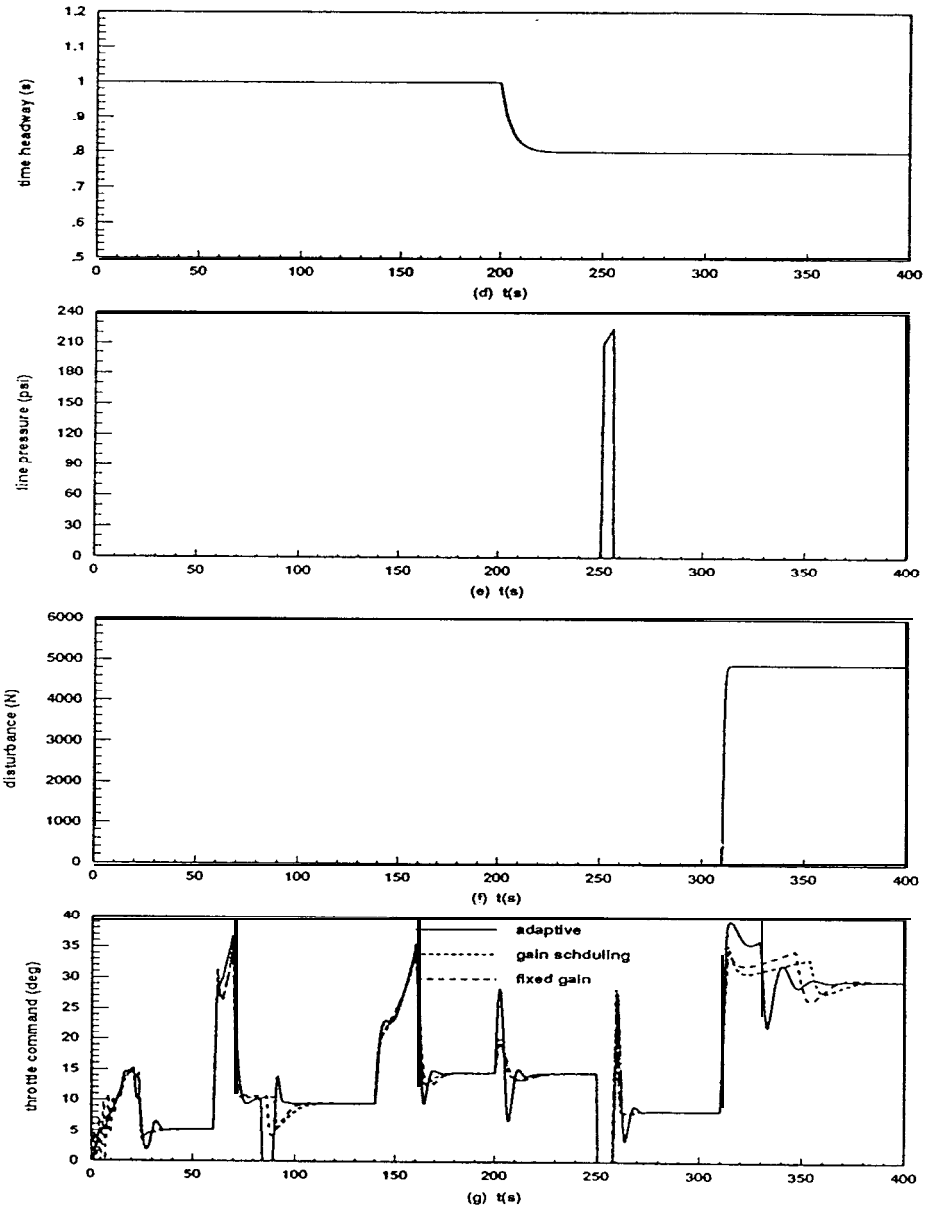

Figure S: (d-g) Simulation results of three controllers

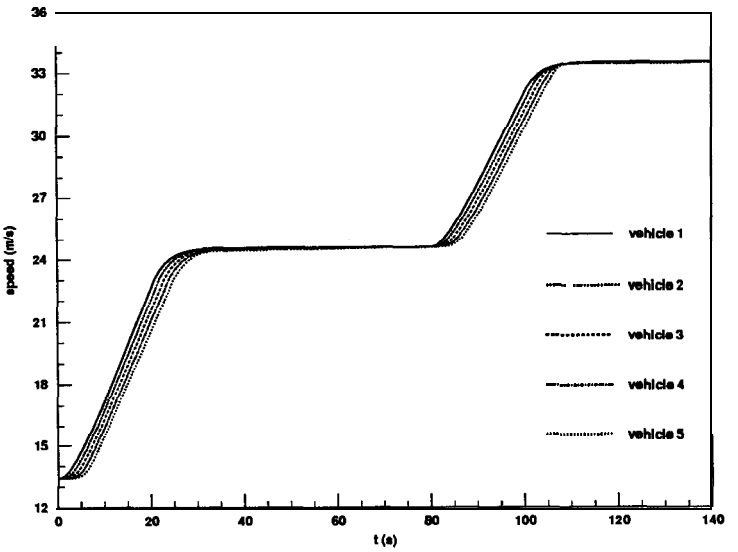

Figure 9: Simulated speed response of 5 vehicle platoon under PID controller with gain scheduling

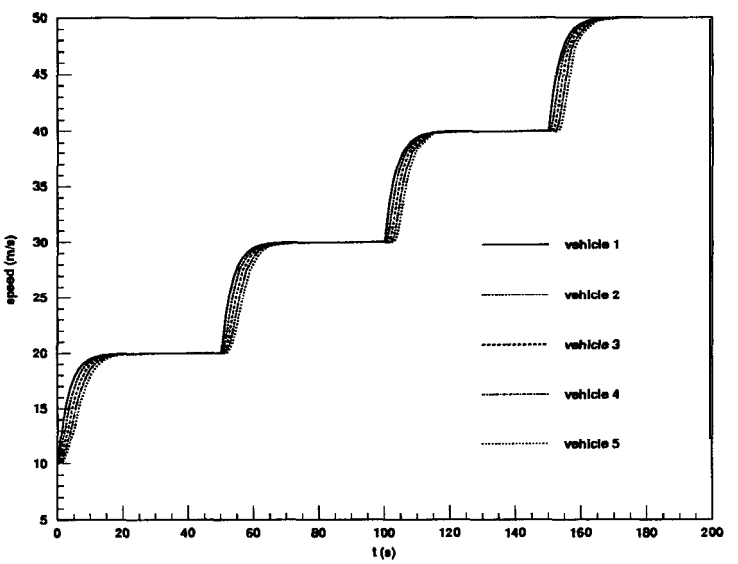

Figure 10: Simulated speed response of 5 vehicle platoon under adaptive controller

PID controller with gain scheduling and the adaptive controller. The results are shown in Figures (9) and (10). It is clear that the speed trajectories are smooth with no speed overshoots.

In addition to the above simulations, the following experiments are performed using actual vehicles. The experiments took place in a test track and were conducted using two vehicles. The leading vehicle was driven manually and in the following vehicle the driver was responsible for steering only.

Experiment 1: Fixed gain PID controller.

The results of the experiment are shown in Figures 11, The controller is turned on at t = 0 second. From $t = 0$ to $t = 86$ second, the speed tracking is good and position error is small even though the leading vehicle's speed and time headway keep changing. Starting at t = 86 second, the leading vehicle accelerates with a large acceleration which exceeds the acceleration limit. Due to the acceleration limiter, the following vehicle accelerates more smoothly and finally catches up with the leading vehicle. Of course, large positive position error (large intervehicle spacing) appears in this case. However, this large positive position error is acceptable since it does not affect the safety and ride comfort.

Experiment 2: Adaptive controller.

The results of the experiment are shown in Figures 12. It is seen that the speed tracking is also good and the position error is small.

In both experiments, we tested the effect of varying the time headway. The time headway was changed by the driver during the experiments. The results show that the performance of the controllers was maintained despite changes in the time headway.

For comparison, we also plot the simulation results in Figures 11 and 12. In the simulation, we took the leading vehicle speed trajectories same as those in the experiments. It can be clearly seen from these two figures that the simulation results and experimental results are very close. The small differences between simulations and experiments may be due to model uncertainty, sensor error, road condition changes, etc. For instance, the test truck is neither straight nor flat. These road condition changes cannot be duplicated in the simulation.

The PID controller with gain scheduling was also tested on the actual vehicle. Its performance is very similar to that of the fixed gain PID controller.

9 Conclusion

In this paper we designed several throttle/brake controllers for automatic vehicle following. The controllers are simulated using a validated nonlinear longitudinal model and tested on actual vehicles. Both the simulations and experiments show that the proposed three controllers achieve good velocity and position tracking without violating the riding comfort

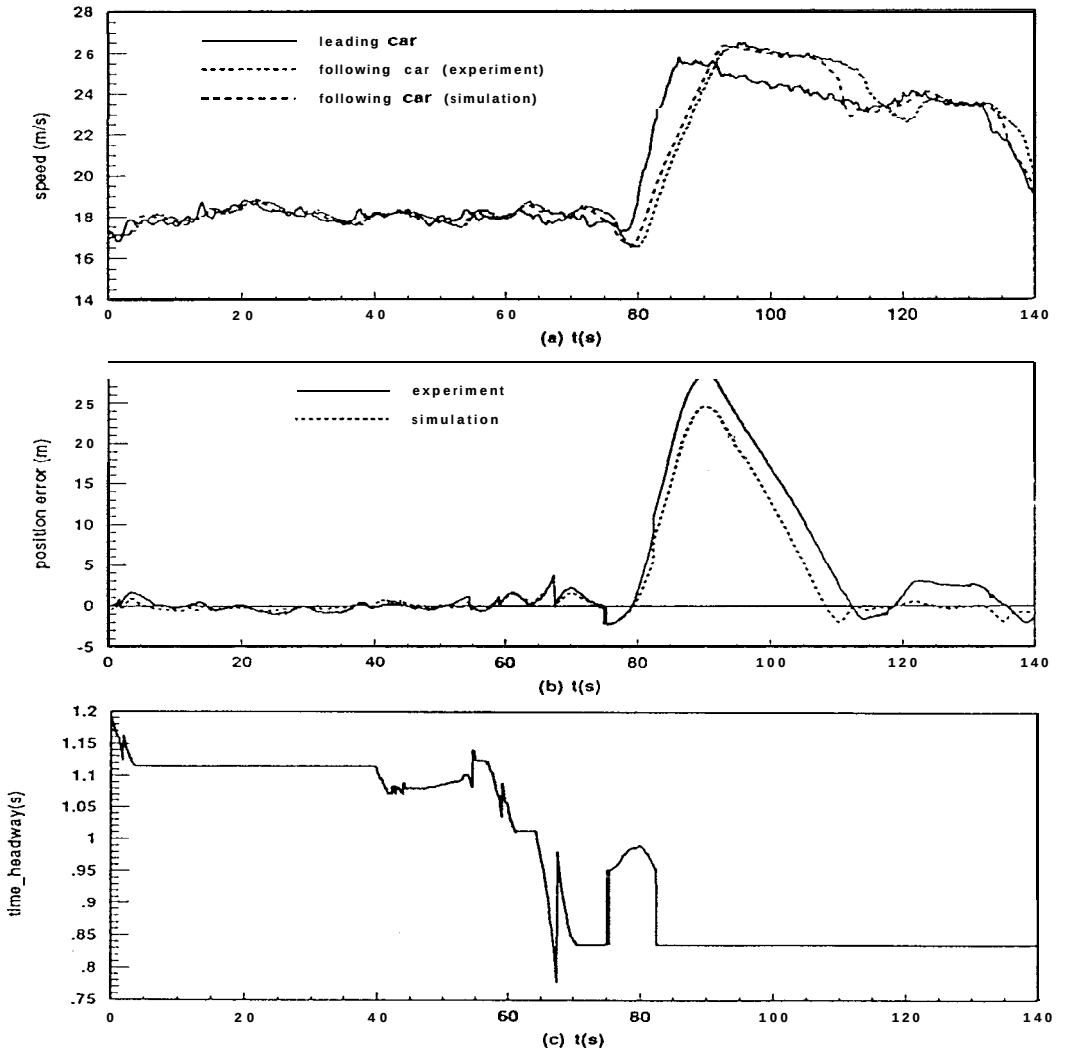

Figure 11: Experimental results of fixed gain PID controller

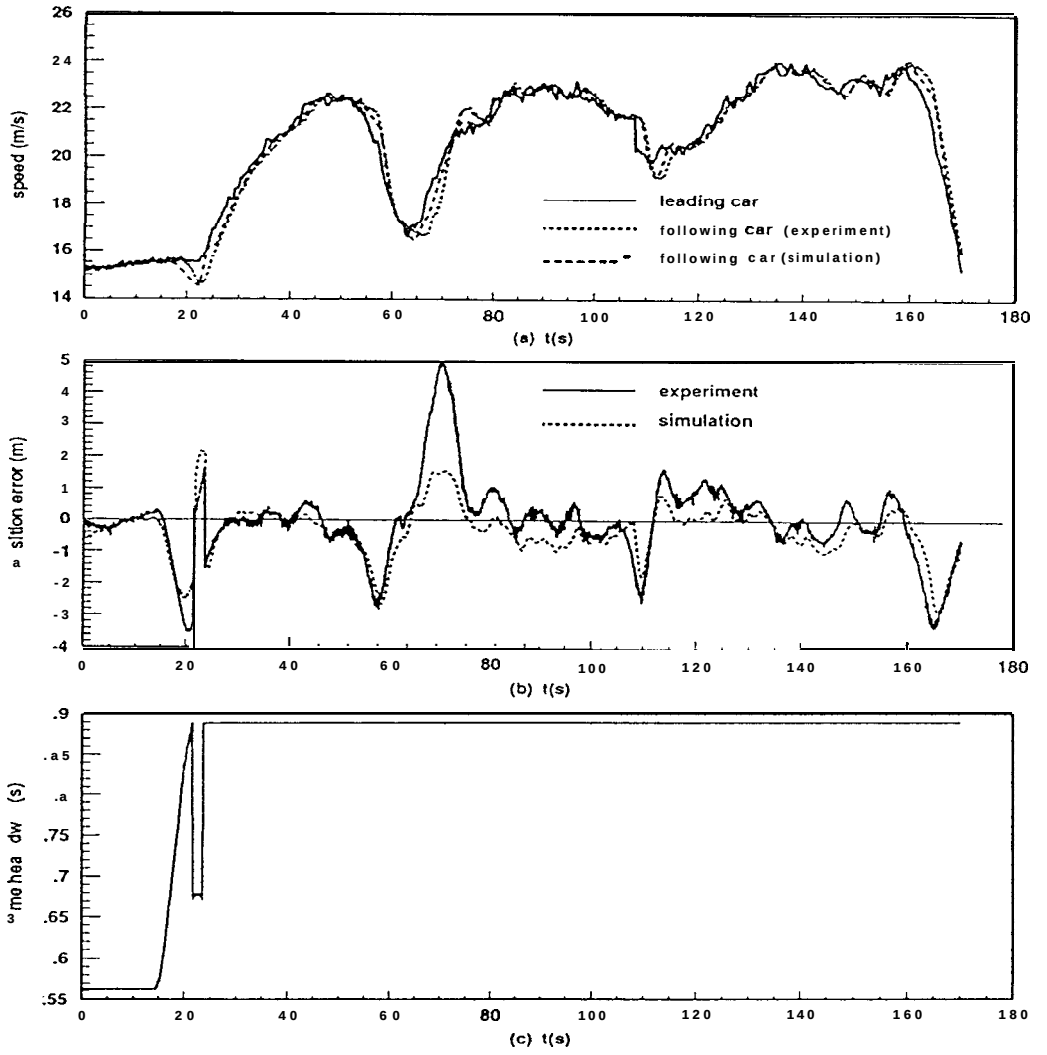

Figure 12: Experimental results of adaptive controller

constraints. The fixed gain PID controller is the simplest one, but it causes some oscillation in acceleration and deteriorates the riding comfort at low speed. The adaptive controller has the fastest response and is somehow vehicle independent, but it requires more calculations. The performance of the PID controller with gain scheduling is between that of the other two controllers. The PID controller with gain scheduling and the adaptive controller are also shown to achieve platoon stability in addition to vehicle stability.

10 Acknowledgments

We would like to thank the Ford researchers: Drs. Mike Shulman, Steve Eckert, Durk Wuh, Farid Ahmed-Zaid, and Mr. David Clemons, Mr. Melvin Palmer, Mr. Tom Sieja, Mr. Mark Pedersen, Mr. William Koehler for their expert explanations and comments regarding vehicle dynamics and control and for their help in doing the road tests. We would also like to thank Mr. Cheng Chih Chien for his help in platoon dynamic analysis.

References

[1] S. E. Shladover, Longitudinal Control of Automotive Vehicles in Close-Formation Platoons, *ASME Journal on Dynamic Systems, Measurement and Control,* vol.113, pp. 231-241, 1991.

[2] S. E. Shladover, C. A. Desoer, J. K. Hedrick, M. Tomizuka, J. Walrand, W. B. Zhang, D. McMahon, H. Peng, S. Sheikholeslam, and N. McKeown, Automatic Vehicle Control Developments in the PATH Program, *IEEE Trans. on Vehicular Technology, vol.* 40, pp. 114-130, 1991.

[3] S. Sheikholeslam and C. A. Desoer, A System Level Study of the Longitudinal Control of a Platoon of Vehicles, *ASME Journal on Dynamic Systems, Measurement, and Control*, *1991.*

[4] P. Varaiya, Smart Cars on Smart Roads: Problems of Control, PATH Technical Memorandum, 91-S, December 1991.

[5] C. C. Chien and P. Ioannou, Automatic Vehicle Following, *Proc. American Control Conference,* Chicago, Il., June 1992.

[6] J. K. Hedrick, D. McMahon, V. Narendran, and D. Swaroop, Longitudinal Vehicle Controller Design for IVHS System, *Proceeding* of American *Control Conference,* June 1991, vol.3, pp. 3107-3112.

[7] Harry Y. Chiu, George B. Stupp, and Samuel J. Brown, Vehicle-Follower Control with Variable-Gains for Short-Headway Automated Guideway Transit Systems, *Journal of Dynamic Systems, Measurement and Control,* Vol. 99, No. 3, Sept., 1977, pp. 183—189.

[8] Alan J. Pue, A State Constrained Approach to Vehicle Follower Control for short Headway Automated Guideway Transit Systems, ***Proceedings of 1977 Joint Automatic Control*** Conference, San Francisco, June, 1977, Vol. 1, pp. 401-407.

[9] S. Sheikholelslam and C. A. Desoer, A system level study of the longitudinal control of a platoon of vehicles, *ASME* Journal ***of Dynamic*** System, ***Measurement and Control,*** 1991.

[10] S. E. Shladover, Operation of automated guideway transit vehicles in dynamically reconfigured trains and platoons, UMTA-MA-060085-79, 1979.

[11] A. S. Hauksdottir and R. E. Fenton, On the Design of a Vehicle Longitudinal Controller, ***IEEE Transaction on Vehicular Technology,*** Vol. VT-34, No. 4, Nv. 1985, pp. 182-187.

[12] B. K. Powell and J. A. Cook, Nonlinear low frequency phenomenological engine modeling and analysis, ***Proceeding of*** American Control ***Conference,*** Minneapolis, MN, June 1987, pp. 332-340.

[13] M. Wiirtenberger, St. Germann, and R. Isermann, Modelling and parameter estimation of nonlinear vehicle dynamics, DSC-Vol 44, ***Transportation Systems,*** 1992, ASME 1992, pp. 53-63.

[14] Z. Xu and P. Ioannou, Modeling of the Brake Line Pressure to Tire Brake Force Subsystem, Techinical Report to PATH and Ford Motor Co., No. 92-09-01, 1992.

[15] P. Ioannou and A. Datta, Robust Adaptive Control: A Unified Approach, *Proc. of the IEEE,* vo1.79, pp. 1736-1769, December 1991.

[16] S. E. Shladover, Longitudinal Control of Automated Guideway Transit Vehicle within Platoons, ASME Journal of Dynamic System, Measurement and Control. Vol. 100, December, 1978.